Particle Design

Generation of Monodisperse Particles by Using Microfluidics: Control over Size, Shape, and Composition**

Shengqing Xu, Zhihong Nie, Minseok Seo, Patrick Lewis, Eugenia Kumacheva, Howard A. Stone, Piotr Garstecki, Douglas B. Weibel, Irina Gitlin, and George M. Whitesides**

Herein we describe a versatile new strategy for producing monodisperse solid particles with sizes from 20 to 1000 μm. The method involves the formation of monodisperse liquid droplets by using a microfluidic device and shaping the droplets in a microchannel and then solidifying these drops in situ either by polymerizing a liquid monomer or by lowering the temperature of a liquid that sets thermally. This method has the following features: 1) It produces particles with an exceptionally narrow range of sizes.[1] 2) A new level of control over the shapes of the particles is offered. 3) The mechanism for droplet formation allows the use of a wide variety of materials including gels, metals, polymers, and polymers doped with functional additives. 4) The procedure can be scaled up to produce large numbers of particles.

A number of methods exist for making inorganic and organic particles with narrow polydispersity. Inorganic colloids are typically prepared by precipitation reactions from organometallic precursors.[2,3] Polymer colloids with sizes from 20 nm to approximately 1 μm are usually prepared by a variation of emulsion polymerization techniques.[4] Larger beads are accessible through miniemulsion polymerization,[5]

[*] Dr. S. Xu, Z. Nie, M. Seo, P. Lewis, Prof. Dr. E. Kumacheva
Department of Chemistry
University of Toronto
80 Saint George Street, Toronto M5S 3H6, Ontario (Canada)
Fax: (+1) 416-978-3576
E-mail: ekumache@chem.utoronto.ca
Dr. P. Garstecki, Dr. D. B. Weibel, I. Gitlin, Prof. Dr. G. M. Whitesides
Department of Chemistry and Chemical Biology
Harvard University
12 Oxford Street, Cambridge, MA 02139-4307 (USA)
Fax: (+1) 617-495-9852
E-mail: gwhitesides@gmwgroup.harvard.edu
Prof. Dr. H. A. Stone
Division of Engineering and Applied Sciences
Harvard University
308 Pierce Hall, Cambridge, MA 02139-4307 (USA)

[**] E.K. acknowledges the Canada Research Chair Fund. Work by P.G., D.B.W., I.G., and G.M.W. was supported by the NIH (GM65364), DoE (DE-FG02-OOER45852), and DARPA, and they used the MRSEC Shared Facilities supported by the NSF under Award No. DMR-9809363. H.A.S. thanks Unilever and Harvard MRSEC (DMR-0213805) for support. P.G. acknowledges the Foundation for Polish Science for a postdoctoral fellowship. D.B.W. thanks the NIH for a postdoctoral fellowship (GM067445). We thank Professor W. C. W Chan for help with the synthesis of CdSe QDs.

Supporting information for this article is available on the WWW under http://www.angewandte.org or from the author.

  DOI: 10.1002/anie.200462226

membrane emulsification,[6] and multistage processes.[7,8] Most of these methods are specific to a particular material. A technique sufficiently general to be applicable to a range of materials and allow the production of monodisperse colloids with control over size and shape has not been demonstrated and would be widely useful.

We have used a new type of microfluidic flow-focusing device (MFFD)[11] to generate droplets of different sizes and shapes and narrow dispersity, and these droplets were solidified in situ. The MFFDs were prepared in either poly(dimethylsiloxane) or polyurethane by using soft lithography;[9,10] an appropriate choice of the material of fabrication allowed us to produce water-in-oil or oil-in-water dispersions. Our experiments suggest that the hydrodynamic mechanism behind the stable and controllable breakup of liquid threads in these MFFDs is largely insensitive to the composition of the dispersed phase. We exploited this property to produce metal particles, microgels, and polymer particles that contain liquid crystals, fluorescent dyes, and inorganic nanoparticles. Control of both the shape and size of the solidified beads was also demonstrated; spheres, disks, ellipsoids, and rods were produced by controlling the volume of the individual drops and the cross-sectional area of the microchannel.

Figure 1a shows the design of the MFFD. A pressure gradient along the long axis of the device forced two immiscible liquids through the orifice of MFFD. The continuous phase was supplied from two sides of the device; the liquid stream comprising the dispersed phase was supplied from a central channel (Figure 1a). The continuous phase surrounds the inner, immiscible liquid so that the inner thread becomes unstable and breaks in the orifice in a periodic manner to release droplets into the outlet channel. We showed recently that the narrow size distribution of gaseous bubbles generated in a similar MFFD is a consequence of the controlled progression of the capillary instability.[12] Owing to viscous retardation in the confinement of the orifice, the velocity of collapse of the thread is reduced[13] and is controlled by the rate of flow of the continuous phase. As a result, the breakup process is much slower than the rates at which the shape of the interface and the liquid pressure fields equilibrate. This mechanism of droplet formation is different to the usual breakup of liquid jets. In contrast to the capillary instability in an unbounded fluid, the breakup in a MFFD produces extremely monodisperse droplets. Furthermore, there are obvious differences with the ink-jet printing technologies that also produce droplets with uniform size distributions. Breakup in ink-jet printers is governed by the competition between surface tension and inertial forces rather than viscous forces, and it occurs in an atmosphere of gas rather than in coflowing, immiscible liquids as in the case of MFFD.

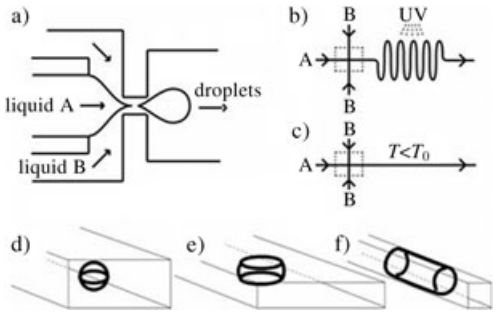

Figure 1. a) A representation of the flow-focusing geometry used in the microfluidic droplet generator. The two immiscible liquids A and B are forced into the narrow orifice where the inner liquid core breaks to release monodisperse droplets into the outlet channel. b), c) Representations of the devices used for producing photochemically and thermally solidified particles. The dashed rectangles mark the flow-focusing device shown in part a). The channels used for photochemical cross-linking were elongated to allow longer durations of exposure of the droplets to UV light. For thermal setting experiments, the flow-focusing region was kept at a temperature exceeding the gelling (or solid–liquid phase transition) temperature (T_0). The outlet channel was cooled to a temperature below T_0, and the droplets solidified as they traveled down the channel. d)–f) Representations of the shapes of drops in the microfluidic channel. If the volume of the droplet exceeds that of the largest sphere which could be accommodated in the channel, the droplet is deformed into a disk (e) or an ellipsoid or rod (f).

We obtained particles by solidifying these droplets either photochemically (by photopolymerization of monomer fluids, see Figure 1b) or thermally (Figure 1c). The volume of the droplets (V) was controlled by the flow rates of the continuous and dispersed phases. The diameter of an undeformed (regular) spherical droplet is given by $d_S = (6V/\pi)^{1/3}$ (Figure 1d). Nonspherical droplets form when d_S is larger than at least one of the dimensions of the outlet channel. In such channels, because of confinement, breakup is not followed by shape relaxation of droplets into spheres. In wide channels, $w > d_S$, (w = width) of height $h < d_S$, the drops assume a discoid shape (Figure 1e) with circular interfaces with the top and bottom walls of the channel. The diameter, d_D, of these interfaces is set by the height of the channel and the volume of the droplet. For channels with small aspect ratios (h/d_D), the droplets have a cylindrical geometry (the curvature at the liquid–liquid interface can be neglected), and the volume of these droplets is $d_D \approx 2(V/\pi h)^{1/2}$. If both the height and the width of the channel are smaller than d_S, the droplet makes contact with all of the channel walls and assumes a rodlike morphology (Figure 1f). The length l_R of elongated liquid plugs yields $l_R \approx V/wh$. The two aspect ratios (h/l_R and w/l_R) can be controlled independently by changing the volume of the droplet and the ratio of the height to the width of the channel.

Polymerization produced monodisperse solid particles from tripropyleneglycol diacrylate (TPGDA), dimethacrylate oxypropyldimethylsiloxane (DMOS), divinylbenzene (DVB), ethyleneglycol diacrylate, and pentaerythritol triacrylate in aqueous suspensions with sodium dodecylsulfate (SDS, 2 wt%) as a surfactant. Monomers were mixed with a photoinitiator, 1-hydroxycyclohexylphenyl ketone (4 wt%), and photopolymerized in a wavy channel (Figure 1b) by illumination with UV light (400 W, $\lambda = 330$–380 nm). The polymerization time was typically between 15 and 800 s. The diameter of the microspheres (controlled by the rates of flow of the water and droplet phases and the geometry of the MFFD) was between 20 and 200 μm. Figure 2a shows a typical SEM image of spherical polyTPGDA beads polymerized in the MFFD; a colloidal crystal formed by these microspheres is illustrated in Figure 2b. We also prepared

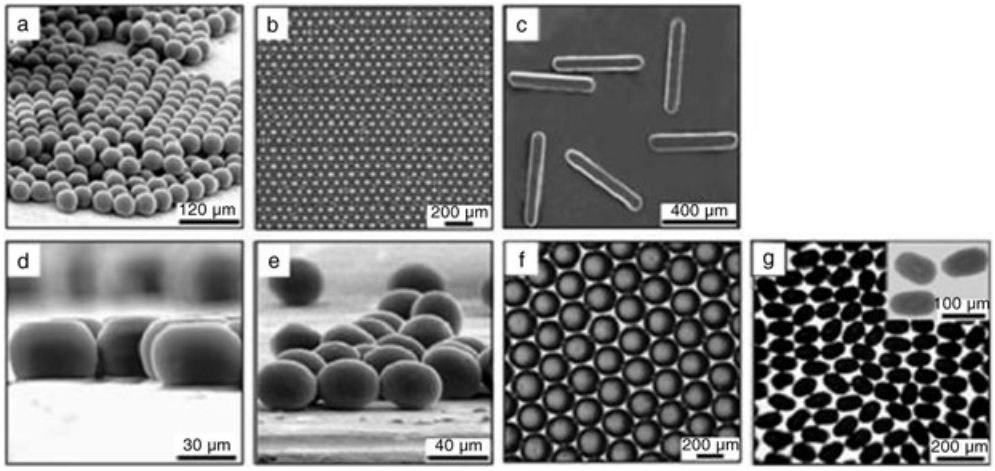

Figure 2. Optical microscopy images of polyTPGDA particles: a) microspheres, b) crystal of microspheres, c) rods, d) disks, and e) ellipsoids. Optical microscopy images of f) agarose disks and g) bismuth alloy ellipsoids produced using thermal solidification; inset: micrograph of the bismuth alloy ellipsoids at higher magnification.

polymeric rods, disks, and ellipsoids by trapping the non-spherical confined monomer droplets (shown in Figure 1e and f) in the solid state. We obtained disks and rods with aspect ratios as large as 1/3 and 1/12 (Figure 2c and d, respectively). Ellipsoids were formed at high flow rates of the continuous phase (Figure 1b).

The conversion of monomer to polymer was close to 100%. Generally, the dimensions of polymer microspheres were 5–10% smaller than the corresponding droplets owing to monomer shrinkage during photopolymerization. A thin wetting layer of the continuous phase prevented clogging of the channels by the solid particles. The rate of microbead production was up to 250 particles s^{-1}. The polydispersity (defined as the standard deviation in the particle diameter divided by the mean particle diameter) of polymerized particles was 1.5% and was similar to the polydispersity of the corresponding spherical droplets.

Figure 3a shows the variation in V with the ratio of the flow rates of the aqueous phase to the monomer phase. Increasing the ratio of flow rates to a value greater than 82 produced smaller, spherical droplets of DVB and TPGDA (filled symbols). Figure 3b–d demonstrates the size distribution of polyTPGDA spheres, disks, and rods. Particle polydispersity in all cases was less than 1.6% (for disks and rods the standard deviation σ of the diameter and length was divided by the mean values of the droplet diameter and length, respectively).

We also obtained particles by thermally-induced gelation or liquid–solid phase transition by operating at a temperature within the fluid-focusing orifice, T_{FF}, that is greater than the temperature for gelation or the liquid–solid phase transition, T_0, and by cooling the outlet channel to a temperature, $T < T_0$, to solidify the droplets (the configuration in Figure 1c). The particles were prepared from two materials: an aqueous solution of agarose ($T_0 = 37\,^{\circ}C$) and a low-melting bismuth alloy ($T_0 = 47\,^{\circ}C$). In both cases we used a continuous phase composed of a 3 wt% solution of surfactant, sorbitan monooleate (span 80), in hexadecane. Figure 2f illustrates agarose disks whose height was predetermined by the height of the channel (30 and 60 μm). By varying the flow rates of the continuous and dispersant phase, disks with diameters from 50 to 250 μm were obtained. The polydispersity of the disks

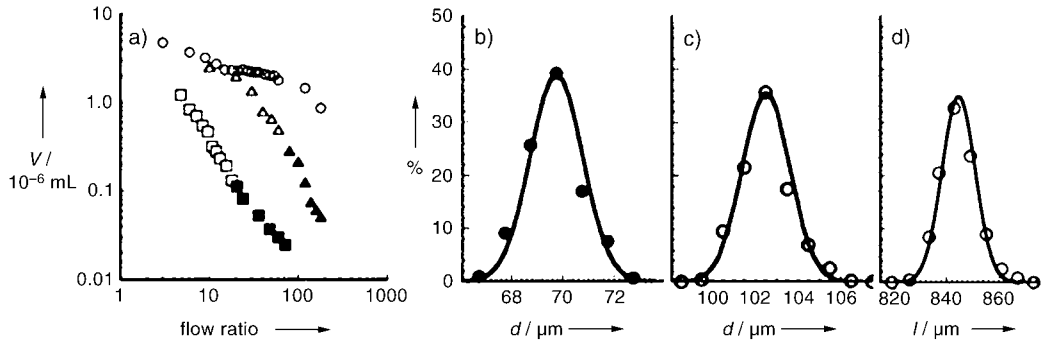

Figure 3. a) A log–log plot of the volume of the droplets versus the ratio of the rates of flow of the aqueous and monomer phases (water:monomer): dimethacrylate oxypropyldimethylsiloxane (circles); divinyl benzene (triangles); TPGDA (squares). The rate of flow of the monomer was 0.04 mL h^{-1}. Open symbols represent disks, filled symbols correspond to spheres. b) and c) Distribution of diameters (d) of poly(TPGDA) spheres and disks, respectively, and d) length (l) of rods. The experimental points were fitted with a Gaussian distribution. The resulting polydispersities are 1.5% for spheres, 1.1% for disks, and 1% for rods.

did not exceed 3%. Figure 2g shows bismuth alloy ellipsoids made in the MFFD geometry illustrated in Figure 1c. The width and the height of the channel were 60 and 60 μm, respectively. The mean width of these ellipsoids was 58 μm (polydispersity 3.2%) and their length was 94 μm (polydispersity 7.8%). The rate of making both agarose and solder particles was controlled by the flow rates applied to the system and ranged between 100 and 1000 particles s^{-1}.

We also produced multicomponent polymer-based beads that include copolymer particles, fluorescent particles containing dyes or nanoparticles, polymer liquid crystals, and microporous particles. Fluorescent microspheres (Figure 4a)

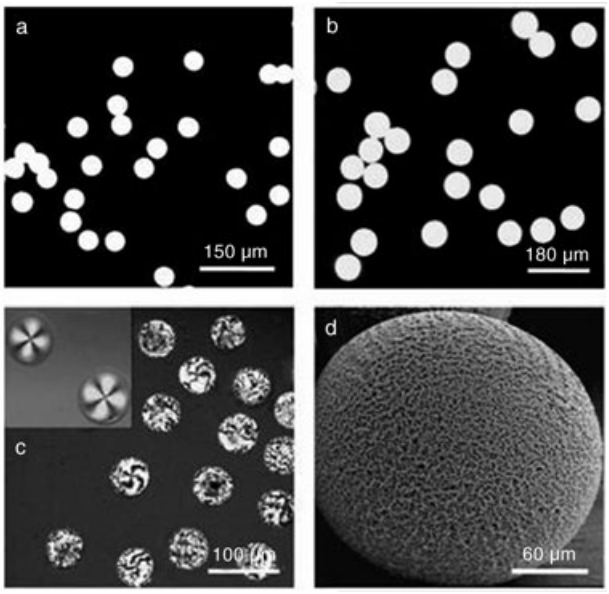

Figure 4. Microspheres labeled with a) NBD dye (NBD = 4-amino-7-nitrobenzo-2-oxa-1,3-diazole, λ_{ex} = 488 nm) and b) CdSe quantum dots (λ_{ex} = 502 nm). c) Polarization microscopy image of 4-cyano-4′-pentylbiphenyl polyTPGDA microspheres. Inset shows particle morphology at low polymerization rate (see text). d) SEM image of a porous polyTPGDA microsphere.

were synthesized by copolymerizing methyl acrylate, which was covalently attached to UV, visible, or near-IR dyes, with TPGDA[14] or by polymerizing TPGDA admixed with 4-nm-diameter CdSe quantum dots (Figure 4b).[15] Other types of hybrid microspheres were obtained by polymerizing monomers mixed with metal or magnetic nanoparticles. We synthesized liquid crystal (LC) polymer microbeads by polymerizing TPGDA admixed with 4-cyano-4′-pentylbiphenyl (5–20 wt%) (Figure 4c). When the polymerization was fast, the LC mixed uniformly with polyTPGDA; when slow, the LC segregated into the core of the microsphere (Figure 3c, inset). Porous microspheres were synthesized by mixing dioctyl phthalate with TPGDA (1/4 wt ratio), followed by polymerization, and subsequent removal of the porogen with acetone (Figure 4d). The mean size of the pores was 0.90 μm.

A single device can produce 10^5–10^6 particles per hour. To increase throughput, we envision making beads by positioning several flow-focusing devices on a single chip. The use of a high-flux UV lamp and more-efficient photoiniators will allow the length of the outlet channel required for polymerization to be decreased. Thereby, it should be straightforward to fit more than 10 devices onto a single 2 × 3-inch substrate. Given that a single MFFD device produces approximately 100–1000 particles sec^{-1}, a multidevice chip will produce about 10^6–10^8 particles h^{-1}.

In summary, the strategy described in the present work has four significant advantages: 1) it offers extensive control over the size and polydispersity of the particles, 2) particles with various shapes can be generated, 3) a range of materials can be applied, including heterogeneous multiphase liquids and suspensions, and 4) useful quantities of particles (up to 10^8 particles h^{-1}) can be produced. Control over the composition of the particles gives access to a variety of material properties. Optically and magnetically functionalized polymeric beads result from polymerization of monomer droplets doped with dyes, semiconductor quantum dots, magnetic nanoparticles, and liquid crystals. This work provides a route to materials for a systematic study of entropically ordered mixtures of particles with different shapes.[16–18]

We believe that the hydrodynamic mechanism governing the breakup of the continuous liquid stream into monodisperse droplets and the processes of thermal solidification and polymerization should both be applicable to the controlled formation of submicron particles.

Received: October 6, 2004
Published online: December 21, 2004

Keywords: copolymerization · gels · microfluidics · monodisperse particles · polymers

[1] According to the standards of the National Institute of Standards and Technology (NIST): "a particle distribution may be considered monodisperse if at least 90% of the distribution lies within 5% of the median size" (*Particle Size Characterization*, Special Publication 960–961, January 2001). To determine the standard deviations, we fit the experimental histograms of the size of the particles with Gaussian distributions. The standard deviations were typically on the order of 1–2% of the mean size, complying with the NIST definition of monodispersity (95% of the particles are within two standard deviations of the mean size).
[2] P. Jiang, J. F. Bertone, V. L. Colvin, *Science* **2001**, *291*, 453–457.
[3] B. T. Holland, C. F. Blanford, A. Stein, *Science* **1998**, *281*, 538–540.
[4] *Colloidal Polymers* (Ed.: A. Elaissari), Marcel Dekker, New York, **2003**.
[5] M. Antonietti, K. Landfester, *Prog. Polym. Sci.* **2002**, *27*, 689–757.
[6] S. Omi, G.-H. Ma, M. Nagai, *Macromol. Symp.* **2000**, *151*, 319–330.
[7] S. T. Eckersley, A. Rudin, *Prog. Org. Coat.* **1994**, *23*, 387–402.
[8] J. S. Song, F. Tronc, M. A. Winnik, *J. Am. Chem. Soc.* **2004**, *126*, 6562–6563.
[9] Y. Xia, G. M. Whitesides, *Angew. Chem.* **1998**, *110*, 568–594; *Angew. Chem. Int. Ed.* **1998**, *37*, 550–575.
[10] D. C. Duffy, J. C. McDonald, O. J. A. Schueller, G. M. Whitesides, *Anal. Chem.* **1998**, *70*, 4974–4984.
[11] S. L. Anna, N. Bontoux, H. A. Stone, *Appl. Phys. Lett.* **2003**, *82*, 364–366.

[12] P. Garstecki, H. A. Stone, G. M. Whitesides, unpublished results.
[13] P. S. Hammond, *J. Fluid Mech.* **1983**, *137*, 363 – 384.
[14] H. Pham, I. Gourevich, J. Oh, J. Jonkman, E. Kumacheva, *Adv. Mater.* **2004**, *16*, 516 – 520.
[15] M. A. Hines, P. Guyot-Sionnest, *J. Phys. Chem. B* **1996**, *100*, 468 – 471.
[16] M. Adams, Z. Dogic, S. L. Keller, S. Fraden, *Nature* **1998**, *393*, *349–352.*
[17] H. N. W. Lekkerkerker, A. Stroobants, *Nature* **1998**, *393*, *305–307.*
[18] M. D. Eldridge, P. A. Madden, D. Frenkel, *Nature* **1993**, *365*, 35 – 37.

